250 m Raster Dataset of Vegetation Classification in the Xizang Autonomous Region Based on FY-3D NDVI (2020)

Zhang, L.[1] Zhou, G. S.[2*] Ren, H. R.[1] Lv, X. M.[2] Ji, Y. H.[2]

1. Department of Geomatics, Taiyuan University of Technology, Taiyuan 030024, China;
2. Chinese Academy of Meteorological Sciences, Beijing 100081, China

Abstract: Understanding the complex vegetation types in the Xizang Autonomous Region is vital for assessing and monitoring ecosystem health. This study developed the 250 m raster dataset of vegetation classification in the Xizang Autonomous Region (2020) utilizing the Google Earth Engine (GEE) platform, the random forest (RF) classification algorithm, and data encompassing terrain, climate, and FY-3D NDVI data. This map, with a 250 m spatial resolution, achieved an overall accuracy (OA) of 81.5% and a Kappa coefficient of 0.79. The results showed that the FY satellite data demonstrates high precision in regional vegetation mapping. This dataset is essential for comprehending the characteristics of Xizang Autonomous Region's vegetation, the ecological changes within the region, and how they respond to climatic factors. The dataset includes: (1) vegetation classification system table, and (2) vegetation distribution data in 250 m raster in 2020. The dataset is archived in .xlsx and .tif formats, and consists of 2 data files with data size of 3.16 MB (compressed to one single file with 2.73 MB).

Keywords: Xizang Autonomous Region; GEE; FY satellite; vegetation map; RF

DOI: https://doi.org/10.3974/geodp.2024.01.05

CSTR: https://cstr.escience.org.cn/CSTR:20146.14. 2024.01.05

Dataset Availability Statement:

The dataset supporting this paper was published and is accessible through the *Digital Journal of Global Change Data Repository* at: https://doi.org/10.3974/geodb.2024.04.07.V1 or https://cstr.escience.org.cn/CSTR:20146.11.2024.04.07.V1.

1 Introduction

Vegetation, referring to the Earth's surface plant communities, plays a pivotal role in maintaining biodiversity, preserving soil stability, and regulating the hydrological cycle, thus

Received: 01-11-2023; **Accepted:** 26-02-2024; **Published:** 25-03-2024

Foundations: Ministry of Science and Technology of P. R. China (2019QZKK0106); Fengyun Satellite Application Advance Plan Program (FY-APP-2022.0309)

***Corresponding Author:** Zhou, G. S. Chinese Academy of Meteorological Sciences, zhougs@cma.gov.cn

Data Citation: [1] Zhang, L., Zhou, G. S., Ren, H. R., *et al*. 250 m Raster dataset of vegetation classification in the Xizang Autonomous Region based on FY-3D NDVI (2020) [J]. *Journal of Global Change Data & Discovery*, 2024, 8(1): 42–50. https://doi.org/10.3974/geodp.2024.01.05. https://cstr.escience.org.cn/CSTR:20146.14.2024.01.05.

[2] Zhang, L., Zhou, G. S., Ren, H. R., *et al*. 250 m raster dataset of vegetation classification in the Xizang Autonomous Region based on FY-3D NDVI (2020) [J/DB/OL]. *Digital Journal of Global Change Data Repository*, 2024. https://doi.org/10.3974/geodb.2024.04.07.V1. https://cstr.escience.org.cn/CSTR:20146.11.2024.04.07.V1.

forming the cornerstone of the planet's environmental health. Vegetation maps, as a representation of vegetation distribution, not only serve as foundational data revealing the patterns and driving factors of surface vegetation distribution but also provide essential information for land management, environmental conservation, and natural disaster prevention.

Recently, remote sensing data from satellites such as Sentinel, Landsat, and the MODIS series has become essential for acquiring land cover/land use information, owing to their high-quality spatio-temporal resolution. Products derived from the Sentinel series, like ESA WorldCover 10m[1] and Sentinel-2 10m Land Use/Land Cover[2], are recognized for their detailed land cover representations. Similarly, Landsat series-based products, including GlobeLand30[3], CLCD[4], and GLC_FCS30[5], play a crucial role in land cover research at both global and regional levels. The MODIS-based MCD12Q1 product[6] is also pivotal in tracking long-term global changes. Contrastingly, the Fengyun-3 (FY-3) satellite, as China's second-generation polar-orbiting climate satellite, provides FY-3D remote sensing data[7]. Compared to remote sensing data from Sentinel, Landsat, and MODIS, FY-3D does not have significant advantages in terms of spatial resolution, spectral resolution, and temporal coverage. Additionally, it lacks support from cloud platforms like Google Earth Engine (GEE) and Pixel Information Expert Engine (PIE-Engine). Therefore, FY-3D data is less commonly used in the field of regional vegetation mapping, and its effectiveness and potential application value still need further validation and exploration.

Located at the center of the Qinghai-Tibet Plateau, the Xizang Autonomous Region is distinguished by its diverse terrain, extreme climate, and unique environment. Understanding the vegetation distribution is vital for local sustainable development and ecological conservation in the region and beyond. This study aims to map the complex vegetation distribution in the Xizang Autonomous Region using FY remote sensing data. The objective is to explore the characteristics and patterns of vegetation in the Xizang Autonomous Region and to evaluate the effectiveness of the FY satellite in regional vegetation mapping tasks.

2 Metadata of the Dataset

The metadata of the 250 m raster dataset of vegetation classification in the Xizang Autonomous Region based on FY-3D NDVI (2020)[8] is summarized in Table 1. It includes the dataset full name, short name, authors, year of the dataset, spatial resolution, data format, data size, data files, data publisher, and data sharing policy, etc.

3 Methods

3.1 Study Area

The Xizang Autonomous Region is located between 26°50′N to 36°53′N and 78°25′E to 99°06′E, with an average altitude of over 4,000 m and a total area of about 1.202,8 million km^2. Known as one of the highest regions in the world, the Xizang Autonomous Region is characterized by a terrain that slopes from northwest to southeast, featuring intersecting mountains and vast plateaus. Influenced by the southern Himalayas, the Xizang Autonomous Region exhibits marked precipitation differences between the northern and southern parts, resulting in a warm and moist climate in the southeast contrasted with a cold and dry climate in the northwest. The vegetation in the Xizang Autonomous Region is varied, encompassing broad-leaved forest, coniferous forest, scrub, meadow, grassland, and desert. The central plateau is predominantly covered with extensive meadow and grassland, whereas the southeast, benefiting from warm and humid conditions, is rich in forest cover. Scrubs are

Table 1 Metadata summary of the 250 m raster dataset of vegetation classification in the Xizang Autonomous Region based on FY-3D NDVI (2020)

Items	Description
Dataset full name	250 m raster dataset of vegetation classification in the Xizang Autonomous Region based on FY-3D NDVI (2020)
Dataset short name	VegetationXizang2020
Authors	Zhang, L., Taiyuan University of Technology, zhanglei1136@link.tyut.edu.cn Zhou, G. S., Chinese Academy of Meteorological Sciences, zhougs@cma.gov.cn Ren, H. R., Taiyuan University of Technology, renhongrui@tyut.edu.cn Lv, X. M., Chinese Academy of Meteorological Sciences, lvxm@cma.gov.cn
Geographical region	Xizang Autonomous Region
Year	2020
Spatial resolution	250 m
Data format	.xlsx, .tif
Data size	3.16 MB (2.73 MB after compression)
Data files	The dataset consists of 2 data files, which includes: (1) vegetation classification system table and (2) vegetation distribution data at 250 m resolution in 2020
Foundation	Ministry of Science and Technology of P. R. China (2019QZKK0106)
Data publisher	Global Change Research Data Publishing & Repository, http://www.geodoi.ac.cn
Address	No. 11A, Datun Road, Chaoyang District, Beijing 100101, China
Data sharing policy	(1) *Data* are openly available and can be free downloaded via the Internet; (2) End users are encouraged to use *Data* subject to citation; (3) Users, who are by definition also value-added service providers, are welcome to redistribute *Data* subject to written permission from the GCdataPR Editorial Office and the issuance of a *Data* redistribution license; and (4) If *Data* are used to compile new datasets, the 'ten percent principal' should be followed such that *Data* records utilized should not surpass 10% of the new dataset contents, while sources should be clearly noted in suitable places in the new dataset[9]
Communication and searchable system	DOI, CSTR, Crossref, DCI, CSCD, CNKI, SciEngine, WDS/ISC, GEOSS

typically found in the area surrounding the central Lhasa River Valley. In the northwest, the region is characterized by its vast desert vegetation, creating a unique desert ecosystem[10, 11].

3.2 Data Sources

In this study, vegetation in the Xizang Autonomous Region was classified into 12 vegetation types: broad-leaved forest, coniferous forest, coniferous and broad-leaved mixed forest, scrub, alpine meadow, alpine grassland, alpine vegetation, alpine desert, cultivated vegetation, wetland, water, and other. This categorization is based on the Vegetation Map of the People's Republic of China (1:1,000,000)[12]. Sample data, comprising 2,774 points, was obtained from 2020 high-resolution Google online imagery (Figure 1). Samples were visually chosen to ensure consistent vegetation types within a 250 m radius around each. These samples, covering various vegetation types, were spread across the study area. As detailed in Table 2, 90% of the samples were used for training, with the remaining 10% reserved for validation.

The remote sensing data used in this study was obtained from the FY-3D MERSI-II 10-day composite vegetation index dataset available through the FENGYUN Satellite Data Center[1], featuring a temporal resolution of 10 days and a spatial resolution of 250 m, encompassing six bands including blue, green, red, near-infrared, NDVI, and EVI. This study selected 36 NDVI images from 2020 as vegetation mapping features. This dataset missing values in areas of water, glacier, and snow cover. Therefore, this study recalculated the NDVI values for these regions using the red and near-infrared bands (Equation1).

[1] FENGYUN Satellite Data Center. https://satellite.nsmc.org.cn.

Table 2 Statistics of training and validation samples for the Xizang Autonomous Region vegetation distribution data at 250 m raster (2020)

Vegetation types	Training samples	Validation samples	Total
Broad-leaved forest	239	27	266
Coniferous forest	120	12	132
Coniferous and broad-leaved mixed forest	79	5	84
Scrub	111	9	120
Alpine meadow	409	44	453
Alpine grassland	490	49	539
Alpine vegetation	166	22	188
Alpine desert	193	26	219
Cultivated vegetation	102	10	112
Wetland	82	8	90
Water	252	35	287
Other	256	28	284
Total	2,499	275	2,774

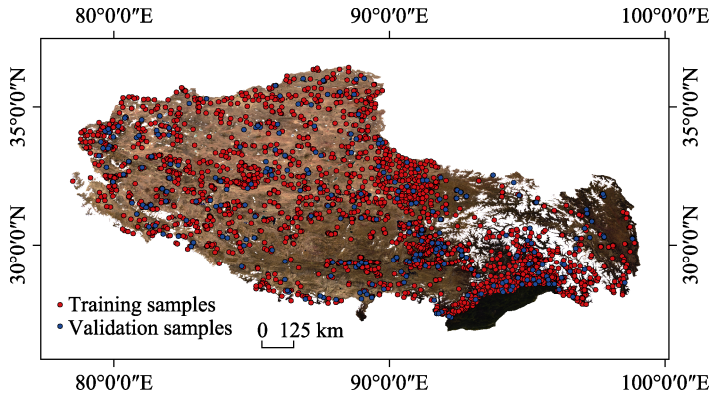

Figure 1 Spatial distribution of training and validation samples for the Xizang Autonomous Region vegetation distribution data at 250 m raster (2020)

$$\mathrm{NDVI} = \frac{\mathrm{NIR} - \mathrm{Red}}{\mathrm{NIR} + \mathrm{Red}} \tag{1}$$

where NIR is the near-infrared band and Red is the red band in FY remote sensing data.

The terrain data for this study was obtained from the Shuttle Radar Topography Mission (SRTM) provided by the USGS[13], with a spatial resolution of 30 m. This data was used to calculate the elevation, slope, and aspect in the Xizang Autonomous Region for vegetation mapping. The climate data, including annual average temperature[14] and annual precipitation[15] for 2020, was sourced from the National Tibetan Plateau / Third Pole Environment Data Center[1] at a spatial resolution of 1,000 m. To achieve consistency across the datasets, the elevation, slope, aspect, annual average temperature, and annual precipitation were resampled to 250 m using the GEE platform.

3.3 Study Methods

3.3.1 GEE Platform and RF Model

The GEE cloud platform is renowned for its robust geospatial data processing capabilities and the comprehensive integration of satellite imagery. Consequently, it has been widely applied in fields such as climate change and environmental monitoring[16]. A variety of machine learning models are compatible with GEE, such as support vector machine (SVM),

[1] National Tibetan Plateau / Third Pole Environment Data Center. https://data.tpdc.ac.cn.

RF, and gradient boosting tree (GBT). In this study, the RF classification model[17] was employed for vegetation mapping. This model operates by randomly selecting samples and features to train each decision tree, thereby enhancing classification accuracy through the combination of predictions from multiple trees. Such an approach effectively minimizes the risk of overfitting and improves the capacity to generalize to new datasets, leading to its widespread use in a range of complex analytical tasks.

3.3.2 Feature Importance Evaluation and Feature Selection

Utilizing a combination of terrain, climate, and remote sensing data, this study developed 41 vegetation mapping features. These features include elevation, slope, aspect, annual average temperature, annual precipitation, and 36 NDVI features derived from the FY3D MERSI-II 10-day composite vegetation index dataset. To prevent model overfitting caused by an excess of features, an approach combining incremental feature selection with minimization of out-of-bag (OOB) error was employed to identify the most effective features for mapping. The process began with assessing the importance of each of the 41 features within the RF model, ranking them from the most to the least importance. Subsequently, models were constructed incrementally, starting with the most important feature and progressively including less significant ones, thus forming various combinations of RF models. The out-of-bag error (OOB error), which is the misclassification rate of the samples not included in the training of each decision tree in the random forest, was calculated for each model. The mapping features corresponding to the model with the lowest OOB error were then utilized in the construction of the final random forest model for vegetation mapping.

3.3.3 Evaluation of Mapping Accuracy

Employing the GEE platform, this study constructed a RF model using the optimal set of features. Combining terrain, climate, and FY-3D NDVI data enabled the creation of the 250 m raster dataset of vegetation classification in the Xizang Autonomous Region (2020). The mapping accuracy was evaluated with the confusion matrix method, which involved calculating the overall accuracy (OA) (Equation 2), Kappa coefficient (Equation 3), producer's accuracy (PA) (Equation 4), and user's accuracy (UA) (Equation 5).

$$OA = \frac{\sum_{i=1}^{n} m_i}{N} \tag{2}$$

$$Kappa = \frac{N \times \sum_{i=1}^{n} m_i - \sum_{i=1}^{n} (G_i \times C_i)}{N^2 - \sum_{i=1}^{n} (G_i \times C_i)} \tag{3}$$

$$PA = \frac{m_i}{G_i} \tag{4}$$

$$UA = \frac{m_i}{C_i} \tag{5}$$

where m_i is the count of correctly classified samples in class i; n represents the total categories; N is the sum of all classified pixels; C_i indicates the pixels classified into class i; G_i is the actual count of pixels in class i; OA is used to denote overall accuracy; Kappa for the Kappa coefficient; PA symbolizes producer's accuracy; UA defines user's accuracy.

3.4 Technical Route

The main development process, as depicted in Figure 2, began with the collection of terrain, climate, and FY-3D NDVI data from 2020, which were resampled to a 250 m resolution. This step generated 41 mapping features, including elevation, slope, aspect, annual average temperature, annual precipitation, and 36 NDVI features from the FY3D MERSI-II 10-day

composite vegetation index dataset. Subsequently, 2,774 representative vegetation samples, selected via visual interpretation from high-resolution Google online imagery, were divided into training (90%) and validation (10%) sets. Utilizing the training set, the study identified an optimal feature set through incremental selection and minimizing OOB error, which then served as the foundation for constructing the RF classification model. This model's effectiveness was assessed using metrics such as OA, UA, PA, and the Kappa coefficient, based on the validation samples. Finally, by employing the developed RF classification model and integrating terrain, climate, and remote sensing data, this study produced the Xizang Autonomous Region vegetation distribution data at 250 m resolution (2020).

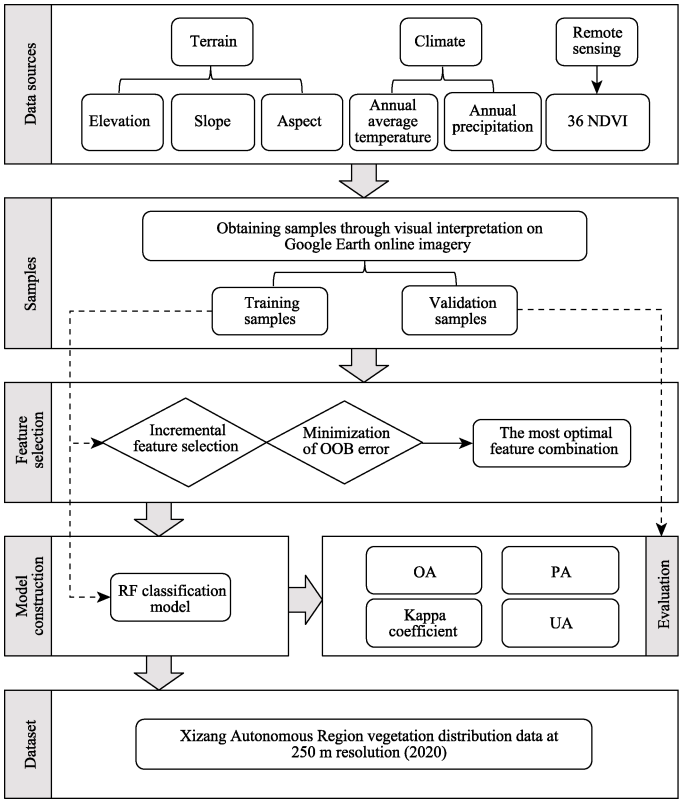

Figure 2 Flowchart of dataset development

4 Data Results and Validation

4.1 Data Results

Incremental feature selection and OOB error minimization were utilized to identify the most effective features for vegetation mapping in this study. Analysis showed that increasing the number of features led to a reduction in OOB error, which reached its minimum of 0.16 with 14 features. However, the error slightly increased to 0.17 as the number of features grew to 41, indicating no further enhancement in model performance beyond 14 features. Therefore, this study identified a set of 14 optimal features for effective mapping: elevation, slope, annual average temperature, annual precipitation, and various NDVI indices (NDVI_0720, NDVI_1020, NDVI_0110, NDVI_0220, NDVI_0310, NDVI_0229, aspect, NDVI_0930, NDVI_1031, and NDVI_0120). Utilizing these features with the RF classification model, vegetation distribution data of the Xizang Autonomous Region with 250 m for 2020 was

produced (Figure 3). The distribution area of each vegetation type in the Xizang Autonomous Region for 2020 was then calculated (Table 3).

Table 3 Distribution area of each vegetation type in the Xizang Autonomous Region in 2020

Vegetation types	Area (km^2)	Vegetation types	Area (km^2)
Broad-leaved forest	49,039.6	Alpine vegetation	136,594.9
Coniferous forest	49,870.5	Alpine desert	154,924.0
Coniferous and broad-leaved mixed forest	7,163.1	Cultivated vegetation	3,834.1
Scrub	10,386.3	Wetland	4,259.3
Alpine meadow	292,323.9	Water	32,169.5
Alpine grassland	404,775.0	Other	63,814.6

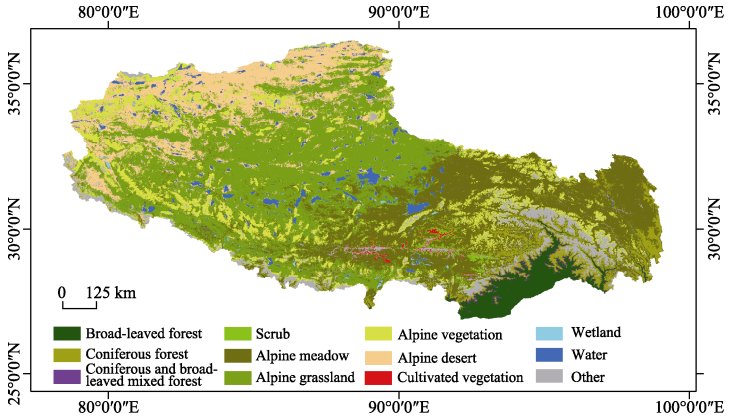

Figure 3 Map of Xizang Autonomous Region vegetation at 250 m raster (2020)

4.2 Data Validation

The Xizang Autonomous Region vegetation distribution data at 250 m resolution (2020) exhibited an overall accuracy of 0.81 and a Kappa coefficient of 0.79, with details of the confusion matrix, PA, and UA provided in Table 4. The UA for coniferous and broad-leaved mixed forest, scrub, alpine meadow, alpine vegetation, and wetland were all below 80%, with coniferous and broad-leaved mixed forest and alpine vegetation specifically at 40.0% and 54.5%, respectively. Furthermore, the UA shows that coniferous and broad-leaved mixed forest, alpine grassland, alpine desert, and cultivated vegetation did not exceed 80%, with coniferous and broad-leaved mixed forest at 50.0%.

According to the confusion matrix, there is noticeable confusion between the broad-leaved forest and coniferous and broad-leaved mixed forest, as well as between alpine grassland and alpine meadow. Coniferous and broad-leaved mixed forest, comprising both broad-leaved and coniferous tree species, exhibit spectral characteristics intermediate to those of broad-leaved and coniferous forests. The phenological changes in broad-leaved trees during spring and autumn, particularly the budding and shedding of leaves, lead to NDVI values that closely resemble those of a broad-leaved forest. This similarity often leads the RF model to misclassify coniferous and broad-leaved mixed forests as broad-leaved forests. Alpine meadows and alpine grassland, both consisting of herbaceous plants, often intertwine in their transition zones, forming ecological transition areas. This intermingling leads to significant similarities in NDVI values in these regions, making the accurate classification of these vegetation types difficult. Alpine vegetation, situated between the treeline or scrub line and the lower limit of the perennial snowline, exhibits low and sparse coverage. Accurately extracting this type of vegetation is a significant challenge due to its

distribution characteristics.

Table 4 Confusion matrix, PA, and UA of the Xizang Autonomous Region vegetation distribution data at 250 m raster (2020)

	Broad-leaved forest	Coniferous forest	Coniferous and broad-leaved mixed forest	Scrub	Alpine meadow	Alpine grassland	Alpine vegetation	Alpine desert	Cultivated vegetation	Wetland	Water	Other	Total number of types	PA
Broad-leaved forest	24	1	2	0	0	0	0	0	0	0	0	0	27	88.9%
Coniferous forest	0	12	0	0	0	0	0	0	0	0	0	0	12	100.0%
Coniferous and broad-leaved mixed forest	3	0	2	0	0	0	0	0	0	0	0	0	5	40.0%
Scrub	0	0	0	6	3	0	0	0	0	0	0	0	9	66.7%
Alpine meadow	0	0	0	1	35	7	0	0	0	1	0	0	44	79.5%
Alpine grassland	0	0	0	0	0	43	0	5	0	0	1	0	49	87.8%
Alpine vegetation	0	0	0	0	2	3	12	0	0	0	0	5	22	54.5%
Alpine desert	0	0	0	0	0	2	1	22	0	0	1	0	26	84.6%
Cultivated vegetation	0	0	0	0	0	0	0	0	9	0	0	1	10	90.0%
Wetland	0	0	0	0	0	0	0	0	0	6	2	0	8	75.0%
Water	0	0	0	0	1	3	0	2	0	0	29	0	35	82.9%
Other	0	0	0	0	0	0	1	0	3	0	0	24	28	85.7%
Total number of types	27	13	4	7	41	58	14	29	12	7	33	30	275	
UA	88.9%	92.3%	50.0%	85.7%	85.4%	74.1%	85.7%	75.9%	75.0%	85.7%	87.9%	80.0%		

5 Discussion and Conclusion

Based on terrain, climate, and FY remote sensing data, this study utilized the GEE platform and the RF model to produce the Xizang Autonomous Region vegetation distribution data at 250 m resolution (2020). This map achieved an OA of 81.5% and a Kappa coefficient of 0.79. The mapping features used in the RF model underscored topography and climate as key determinants of vegetation distribution in the Xizang Autonomous Region. Among these features, elevation, slope, annual average temperature, and annual precipitation were the most influential. The study revealed that ranging from forest, scrub, alpine meadow, and alpine grassland to alpine desert from southeast to northwest, and alpine grassland and scrub to alpine vegetation with increasing altitude. Moreover, this vegetation distribution data achieved high accuracy using FY-3D MERSI-II NDVI data, a contrast to distribution data typically reliant on satellite data from Sentinel, Landsat, and MODIS. This highlights the potential of China's FY satellite in the realm of vegetation mapping.

In summary, this dataset not only reveals a more detailed vegetation distribution in the Xizang Autonomous Region but also validates the potential of domestic FY satellite in regional vegetation mapping. It should be noted, however, that in areas with transitional vegetation, as well as regions where vegetation is dispersed and fragmented, the 250 m spatial resolution may lead to overlap in spectral information and mixed pixel phenomena.

Author Contributions

Zhou, G. S. and Ren, H. R. designed the algorithms of dataset. Lv, X. M. and Ji, Y. H.

performed data validation. Zhang, L. collected, processed the data, and wrote the data paper.

Conflicts of Interest

The authors declare no conflicts of interest.

References

[1] Venter, Z. S., Barton, D. N., Chakraborty, T., *et al*. Global 10 m land use land cover datasets: A comparison of dynamic world, world cover and esri land cover [J]. *Remote Sensing*, 2022, 14(16): 4101.

[2] Karra, K., Kontgis, C., Statman-Weil, Z., *et al*. Global land use/land cover with Sentinel 2 and deep learning [C]. 2021 IEEE international geoscience and remote sensing symposium IGARSS. Institute of Electrical and Electronics Engineers, 2021: 4704–4707.

[3] Chen, J., Ban, Y., Li, S. Open access to Earth land-cover map [J]. *Nature*, 2014, 514(7523): 434–434.

[4] Yang, J., Huang, X. The 30 m annual land cover dataset and its dynamics in China from 1990 to 2019 [J]. *Earth System Science Data*, 2021, 13(8): 3907–3925.

[5] Zhang, X., Liu, L., Chen, X., *et al*. GLC_FCS30: Global land-cover product with fine classification system at 30 m using time-series Landsat imagery [J]. *Earth System Science Data*, 2021, 13(6): 2753–2776.

[6] Friedl, M. A., McIver, D. K., Hodges, J. C., *et al*. Global land cover mapping from MODIS: algorithms and early results [J]. *Remote sensing of Environment*, 2002, 83(1/2), 287–302.

[7] Gao, H., Tang, S. H., Han, X. Z. China's Fengyun (FY) meteorological satellites, development and applications [J]. *Science & Technology Review*, 2021, 39(15): 9–22.

[8] Zhang, L., Zhou, G., Ren, H., *et al*. 250 m raster dataset of vegetation classification in the Xizang Autonomous Region based on FY-3D NDVI (2020) [J/DB/OL]. *Digital Journal of Global Change Data Repository*, 2024. https://doi.org/10.3974/geodb.2024.04.07.V1. https://cstr.escience.org.cn/CSTR:20146.11.2024.04.07.V1.

[9] GCdataPR Editorial Office. GCdataPR Data Sharing Policy [OL]. https://doi.org/10.3974/dp.policy.2014.05 (Updated 2017).

[10] Zhou, G. S., Ren, H. R., Liu, T., *et al*. A new regional vegetation mapping method based on terrain-climate-remote sensing and its application on the Qinghai-Xizang Plateau [J]. *Science China Earth Sciences*, 2023, 53(2): 227–235.

[11] Zhou, G. S., Ren, H. R., Liu, T., *et al*. Vegetation map of Qinghai Tibet Plateau in 2020 with 10 m spatial resolution [DB/OL]. National Tibetan Plateau / Third Pole Environment Data Center, 2022.

[12] Editorial Board of the Vegetation Map of China, Chinese Academy of Sciences. Vegetation and Its Geographical Pattern in China-description of Vegetation Map of the People's Republic of China [M]. Beijing: Geology Publishing House, 2007.

[13] Rabus, B., Eineder, M., Roth, A., *et al*. The shuttle radar topography mission—a new class of digital elevation models acquired by spaceborne radar [J]. *ISPRS Journal of Photogrammetry and Remote Sensing*, 2003, 57(4): 241–262.

[14] Peng, S. Z. 1-km monthly mean temperature dataset for China (1901–2022) [DB/OL]. National Tibetan Plateau / Third Pole Environment Data Center, 2019.

[15] Peng, S. Z. 1-km monthly precipitation dataset for China (1901–2022) [DB/OL]. National Tibetan Plateau / Third Pole Environment Data Center, 2020.

[16] Johansen, K., Phinn, S., Taylor, M. Mapping woody vegetation clearing in Queensland, Australia from Landsat imagery using the Google Earth Engine [J]. *Remote Sensing Applications*: *Society and Environment*, 2015, 1: 36–49.

[17] Biau, G. Analysis of a random forests model [J]. *The Journal of Machine Learning Research*, 2012, 13: 1063–1095.